Supporting information

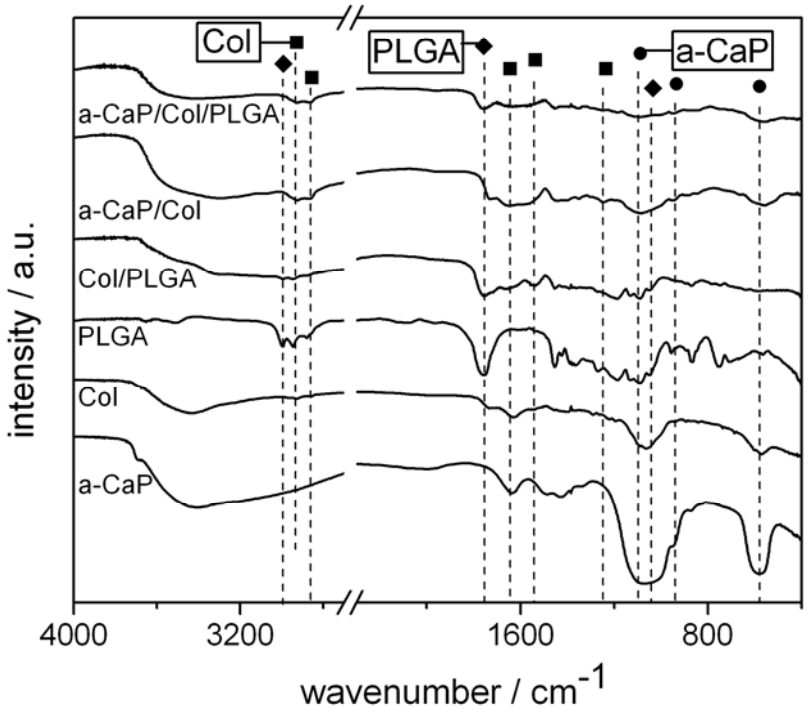

Figure S1: Scaffold components and as prepared scaffolds were investigated by means of Fourier transform infrared spectroscopy: a-CaP, Col, PLGA, Col/PLGA (60/40), a-CaP/Col (60/40), a-CaP/Col/PLGA (70/30/20).

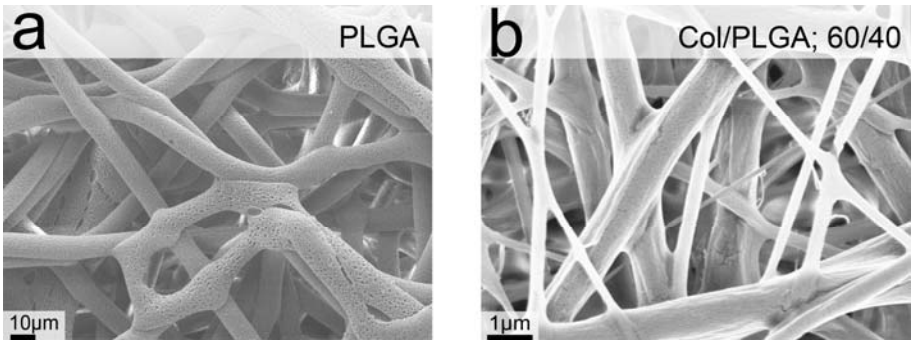

Figure S2: The structure and morphology of fibres without a-CaP nanoparticles is shown by means of scanning electron micrographs. Smooth fibres were obtained for PLGA (a) and Col/PLGA (60/40) (b).

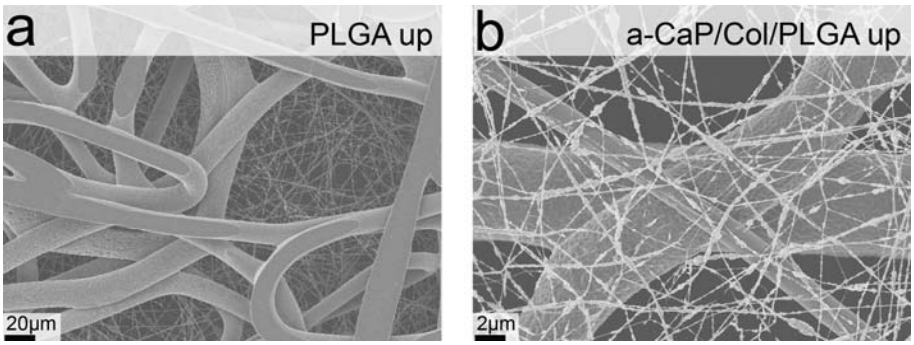

Figure S3: The interface of the double membrane layers was investigated by means of scanning electron microscopy with PLGA fibres in front of the a-CaP/Col/PLGA fibres in (a) and a-CaP/Col/PLGA fibres in front of the PLGA fibres in (b).

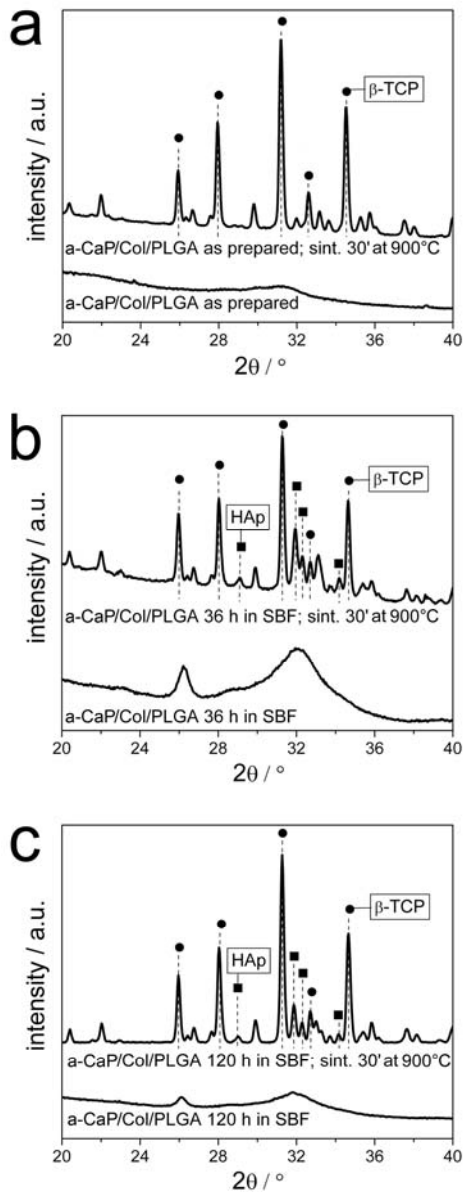

Figure S4: X-ray diffraction patterns of a-CaP/Col/PLGA scaffolds before and after sintering for 30 min at 900°C were recorded. The effect of immersion time in simulated body fluid (SBF) was investigated with a time line that ranges from as prepared (a) over 36 h (b) to a final immersion time of 120 h (c). After immersion in SBF the sintered samples presented not only the characteristic β-TCP phase (26.0°, 28.1°, 31.4°, 32.8°, 34.6°) but also the hydroxyapatite (HAp) phase (28.7°, 31.8°, 32.1° 34.2°).

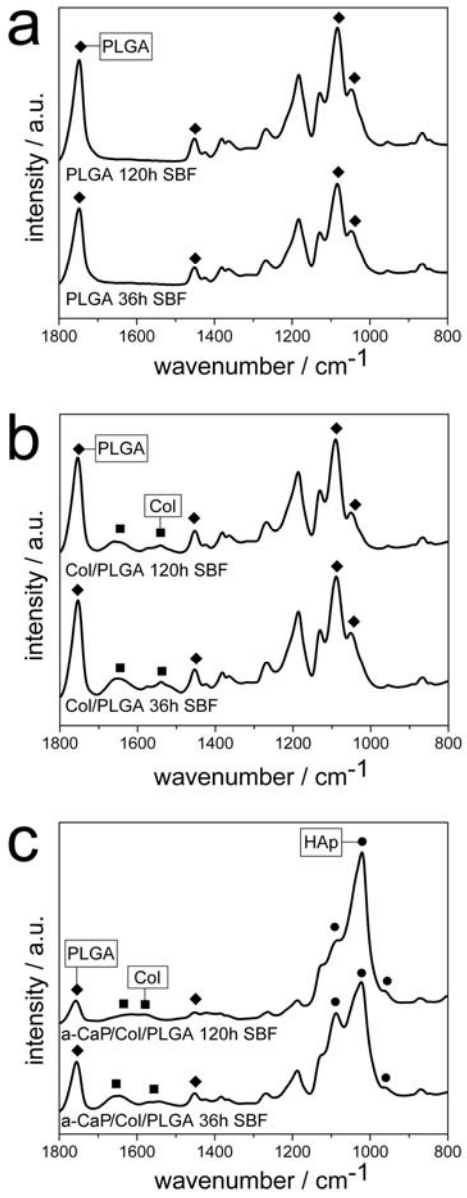

Figure S5: Attenuated total reflection infrared spectra of scaffolds were recorded after immersion in simulated body fluid (SBF) for 36 h and 120 h. In (a) C=O stretching band at 1750 cm^{-1}, C-H stretching at 1450 cm^{-1}, O-C-O stretching at 1080 cm^{-1} and C-CH_3 stretching at 1040 cm^{-1} of PLGA were observed. In (b) additionally the amide I band at 1650 cm^{-1} and the amide II band at 1530 cm^{-1} of collagen in Col/PLGA (60/40) appeared. In (c) the formation of hydroxyapatite (HAp) upon immersion in SBF of a-CaP/Col/PLGA (70/30/20) was demonstrated by PO_4^- stretching bands at 1090 cm^{-1}, at 1050 cm^{-1} and at 960 cm^{-1}.

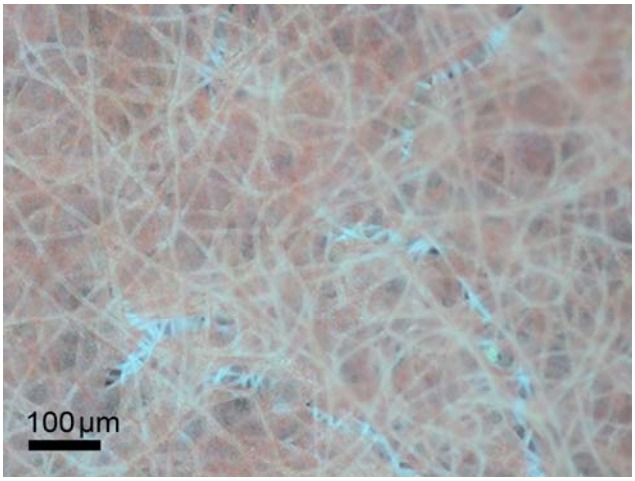

Figure S6: The Sirius red assay of a scaffold with its a-CaP/Col/ATCP side up during cell culture in osteogenic medium for 1 week shows that the a-CaP/Col/PLGA layer (stained in red) was ruptured and partly removed during the course of the cell culture study.

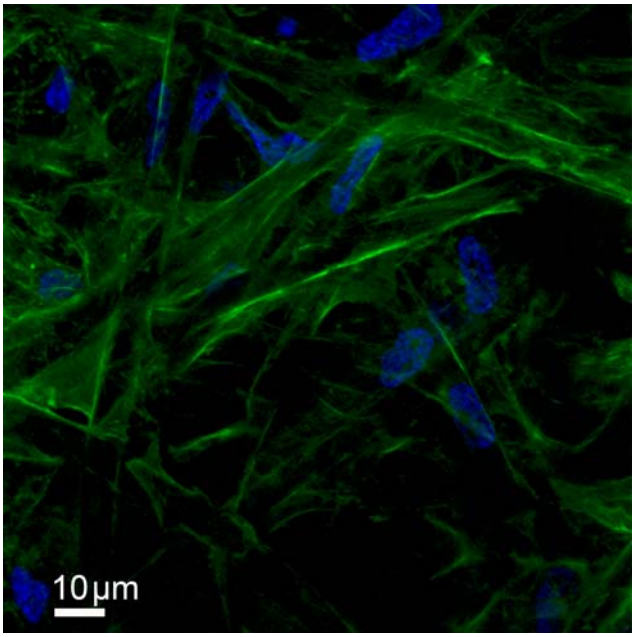

Figure S7: The confocal laser scanning micrograph of a scaffold with its a-CaP/Col/PLGA side up during cell culture in osteogenic medium for 4 weeks illustrates that the PLGA fibres, visible in the fissure of the a-CaP/Col/PLGA layer, have cells adhered on them. This micrograph shows a magnification of the fissure indicated in Figure 10b.

Table S1: Electrospinning parameters for the synthesis of nanofibres at room temperature

	weight ratio a-CaP:Col:PLGA	voltage / kV	feeding rate / mL h^{-1}	distance: needle tip to collector / cm	solvent and concentration	relative humidity / %
pure PLGA	0 : 0 : 100	20	4	20	8 wt% PLGA in chloroform	55
Col/PLGA	0 : 60 : 40	20	1.5	20	4 wt% PLGA in HFIP 8 wt% Col in HFIP	40
a-CaP/Col	20 : 80 : 0	20	0.8	15	8 wt% Col in HFIP 4 wt% a-CaP in HFIP	40
	60 : 40 : 0	20	0.8	15	8 wt% Col in HFIP 4 wt% a-CaP in HFIP	50
a-CaP/Col/PLGA	70 : 30 : 20	20	1.5	20	8 wt% Col in HFIP 4 wt% a-CaP in HFIP	50

Table S2: Fibre diameters as a function of their composition

	weight ratio a-CaP:Col:PLGA	diameter / nm ± standard deviation (n = 100)
pure PLGA	0 : 0 : 100	5980 ± 1220
Col/PLGA	0 : 60 : 40	380 ± 190
a-CaP/Col	20 : 80 : 0	160 ± 120
	60 : 40 : 0	not measurable[‡]
a-CaP/Col/PLGA	70 : 30 : 20	200 ± 90

[‡] As no clear fibre structure could be identified (see Figure 2b), no diameter could be determined.